Macromolecular Rapid Communications
www.mrc-journal.de

Construction of Zwitterionic Coatings with Lubricating and Antiadhesive Properties for Invisible Aligner Applications

Rufang Wei, Junjie Deng, Xiangshu Guo, Yanyu Yang, Jiru Miao, Ashuang Liu, Haiyang Chai, Xinqi Huang, Zhihe Zhao, Xiao Cen, and Rong Wang**

Invisible aligners have been widely used in orthodontic treatment but still present issues with plaque formation and oral mucosa abrasion, which can lead to complicated oral diseases. To address these issues, hydrophilic poly(sulfobetaine methacrylate) (polySBMA) coatings with lubricating, antifouling, and antiadhesive properties have been developed on the aligner materials (i.e., polyethylene terephthalate glycol, PETG) via a simple and feasible glycidyl methacrylate (GMA)-assisted coating strategy. Poly(GMA-*co*-SBMA) is grafted onto the aminated PETG surface via the ring-opening reaction of GMA (i.e., "grafting to" approach to obtain G-*co*-S coating), or a polySBMA layer is formed on the GMA-grafted PETG surface via free radical polymerization (i.e., "grafting from" approach to obtain G-*g*-S coating). The G-*co*-S and G-*g*-S coatings significantly reduce the friction coefficient of PETG surface. Protein adsorption, bacterial adhesion, and biofilm formation on the G-*co*-S- and G-*g*-S-coated surfaces are significantly inhibited. The performance of the coatings remains stable after storage in air or artificial saliva for 2 weeks. Both coatings demonstrate good biocompatibility in vitro and is not caused irritation to the oral mucosa of rats in vivo over 2 weeks. This study proposes a promising strategy for the development of invisible aligners with improved performance, which is beneficial for oral health treatment.

1. Introduction

As living standards rise and people pursue an improved aesthetic, orthodontic treatment for enhancing the alignment and appearance of the teeth is becoming a popular option. In comparison to traditional fixed aligners, invisible aligners provide greater aesthetic appeal and are more comfortable throughout the course of treatment.[1,2] The global market for invisible aligners is expected to grow from 3.1 billion in 2021 to 11.6 billion by 2027, with a compound annual growth rate of 13%.[1] However, the use of aligners can alter the oral ecosystem, leading to a noteworthy rise in the quantity of bacteria linked to caries, like *Streptococcus mutans* (*S. mutans*).[3,4] These bacteria can accumulate on the surface, creating plaque and ultimately resulting in enamel demineralization, periodontitis, and other negative bacterial-related impacts on orthodontic treatment.[3,5,6] In addition, invisible aligners can cause oral mucosal inflammation, mouth ulcers, and other issues due to frequent rubbing during speaking and chewing.[7,8]

Construction of functional coatings has been proposed to endow the device with desirable antibacterial properties to reduce bacterial accumulation on the aligner surfaces. For example, biocides, such as gold nanoparticles,[9] gold nanoclusters,[10,11] and quaternary ammonium salts[12] have been employed to confer aligner surfaces with antibacterial properties. However, the gold nanocomposites would alter the aligners' transparency, which might affect

R. Wei, J. Deng, X. Guo, Y. Yang, J. Miao, A. Liu, H. Chai, R. Wang
Laboratory of Advanced Theranostic Materials and Technology
Ningbo Institute of Materials Technology and Engineering
Chinese Academy of Sciences
Ningbo 315201, P. R. China
E-mail: rong.wang@nimte.ac.cn

R. Wei, J. Deng, X. Guo, Y. Yang, J. Miao, A. Liu, H. Chai, R. Wang
Zhejiang International Scientific and Technological Cooperative Base of Biomedical Materials and Technology
Ningbo Cixi Institute of Biomedical Engineering
Ningbo 315300, P. R. China

R. Wei, J. Deng, Y. Yang, A. Liu, H. Chai, R. Wang
Cixi Biomedical Research Institute
Wenzhou Medical University
Zhejiang 325035, P. R. China

X. Guo
Department of Radiology
The Fifth Affiliated Hospital of Sun Yat-Sen University
Zhuhai 519000, P. R. China

X. Huang, Z. Zhao, X. Cen
State Key Laboratory of Oral Diseases
National Clinical Research Center for Oral Diseases
West China Hospital of Stomatology
Sichuan University
Chengdu 610041, P. R. China
E-mail: cenx@scu.edu.cn

The ORCID identification number(s) for the author(s) of this article can be found under https://doi.org/10.1002/marc.202400234

DOI: 10.1002/marc.202400234

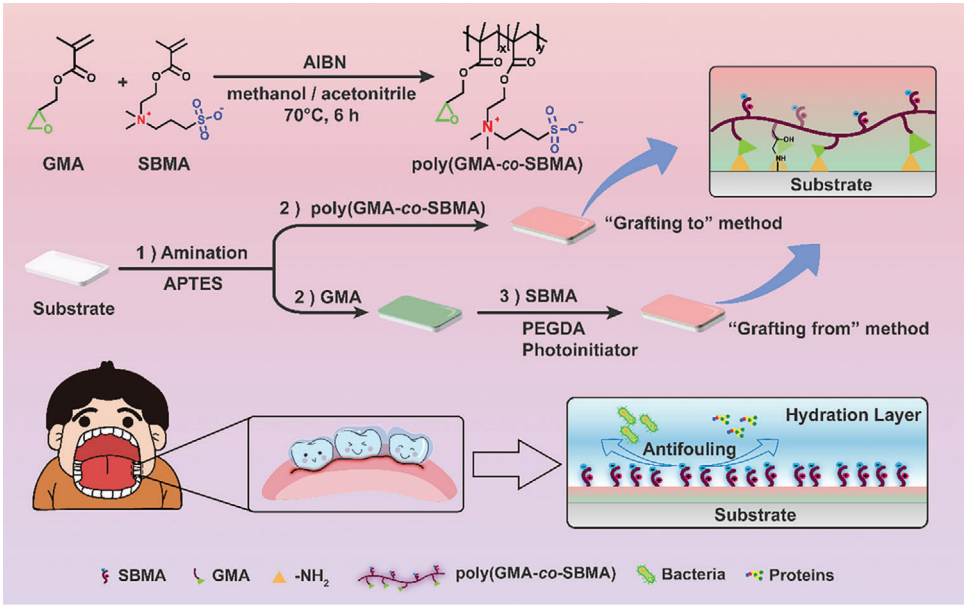

Scheme 1. Schematic diagram of the synthesis process of poly(GMA-*co*-SBMA) and preparation and application of G-*co*-S and G-*g*-S coatings.

their aesthetics. More importantly, biocides could cause an imbalance in the oral ecosystem by indiscriminately killing bacteria, as well as increase concerns about bacterial resistance. On the other hand, the construction of an antifouling coating could reduce protein adsorption and bacterial accumulation on the surface, thus maintaining a clean aligner during the usage.[5,13,14] For instance, Park et al. developed a crosslinked polysaccharide-based multilayer coating containing carboxymethylcellulose and chitosan to prevent bacterial adhesion on invisible aligners.[14] More recently, Xin et al. combined hydrophilic zwitterionic trimethylamine *N*-oxide and hydrophobic antimicrobial ingredient triclosan acrylic in the coating to confer both antimicrobial and antifouling properties to the dental materials.[5] However, most of the conventional coating processes are complicated and not feasible for aligner applications. In addition, the performance of the surface friction of invisible aligners was usually neglected in previous studies.

Coatings with hydrophilic polymers, such as zwitterionic poly(sulfobetaine methacrylate) (polySBMA) have been proposed to reduce surface friction and inhibit protein adsorption, bacterial adhesion, and biofilm formation by forming a hydration layer on the surface, and have been widely used in biomedical applications due to their excellent biocompatibility.[15] Conventional methods of construction of zwitterionic polymer coatings, such as layer-by-layer technique,[16,17] dopamine-assisted immobilization,[18,19] and diffusion-induced interfacial polymerization[20–22] have been proposed. However, these methods are usually not suitable for coating the thermoplastic materials used for invisible aligners (i.e., polyethylene terephthalate glycol, PETG) due to the low coating stability, the high sensitivity of PETG to harsh conditions, such as elevated temperatures and organic solvents,[23,24] and the high aesthetic requirement of invisible aligners. A mild and feasible approach to constructing a stable and transparent hydrophilic coating without affecting the mechanical properties of the aligner materials is highly desirable. Glycidyl methacrylate (GMA) contains an epoxy group, which can react with amino groups via the one-step nucleophilic attack-induced ring-opening reaction and be anchored to the aminated substrate surface, and a vinyl group, which can participate in the free radical polymerization with monomers to form a functional polymer layer.[25,26] The entire GMA-assisted fabrication process could be performed through simple immersion under mild reaction condition to form a robust and stable coating on various substrate surfaces.[27]

In this work, hydrophilic polySBMA coatings with lubricating and antiadhesive properties have been constructed on the surface of invisible aligner materials via the GMA-assisted coating strategy through either "grafting to" or "grafting from" approaches (**Scheme 1**). Hydrophilic poly(glycidyl methacrylate-*co*-sulfobetaine methacrylate) (poly(GMA-*co*-SBMA)) polymer was grafted onto aminated PETG surface via the ring-opening reaction of GMA ("grafting to" approach), or polySBMA was formed via free radical polymerization on GMA-grafted PETG surface ("grafting from" approach). The chemical elements, thickness, hydrophilicity, surface roughness, transparency, and stability of the coatings obtained from both approaches were characterized. The mechanical properties of the coated PETG materials, as well as the lubricity and antifouling and antiadhesive properties of the coatings, were evaluated. In addition, the in vitro biocompatibility and long-term in vivo performance of the coated materials in the oral cavity of rats were investigated.

2. Results and Discussion

2.1. Synthesis and Characterization of Poly(GMA-*co*-SBMA)

In this study, poly(GMA-*co*-SBMA) was synthesized from azobisisobutyronitrile (AIBN)-initiated copolymerization of GMA and SBMA (**Figure 1a**). The molecular weight of poly(GMA-*co*-SBMA) was determined to be 61.2 kDa. The Fourier transform infrared (FT-IR) spectra of poly(GMA-*co*-SBMA), SBMA,

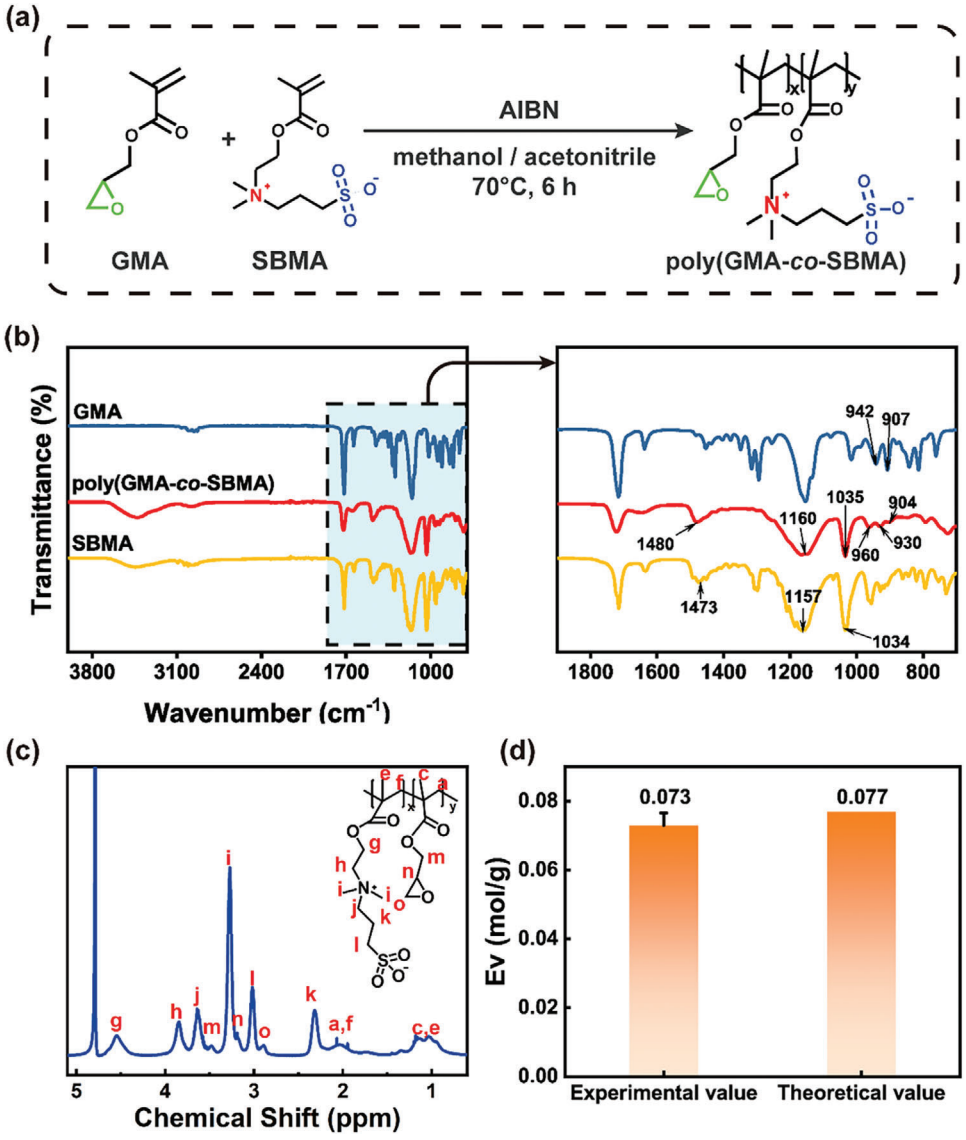

Figure 1. Synthesis and characterization of poly(GMA-*co*-SBMA). a) Schematic illustration of synthesis of poly(GMA-*co*-SBMA). b) FT-IR spectra of SBMA, GMA, and poly(GMA-*co*-SBMA). c) ^{1}H NMR spectrum of poly(GMA-*co*-SBMA). d) Experimental and theoretical epoxy values in poly(GMA-*co*-SBMA).

and GMA were shown in Figure 1b. The peaks at 1160 and 1035 cm^{-1} of poly(GMA-*co*-SBMA) are attributed to the asymmetric and symmetric stretching vibrations of the sulfonate group of SBMA units, the peaks at 960, 930, and 904 cm^{-1} are attributed to the epoxy groups, and the peaks at 1480 cm^{-1} are attributed to the quaternary ammonium groups. The chemical structures of poly(GMA-*co*-SBMA) were further analyzed using ^{1}H nuclear magnetic resonance (^{1}H NMR) (Figure 1c). The resonance signal at 3.84 ppm corresponded to —CH_2— in the polySBMA segment, and the peak at 2.89 ppm corresponded to methylene of the epoxy group (—CH—O—CH_2—) in the polyGMA segment. From the ^{1}H NMR results, it could be calculated that the ratio of polyGMA in the copolymer is ≈18.9% (area ratio of —CH_2— peak to that of —CH—O—CH_2— peak), which is close to the feeding molar ratio of GMA in the monomer (20%). The epoxy ratio of the copolymer was determined to be 0.073 using the hydrochloric acid-acetone titration method, which was close to the theoretical value of 0.077 (Figure 1d). The results above confirmed that the poly(GMA-*co*-SBMA) was successfully synthesized, and the epoxy groups were well preserved in the copolymer.

2.2. Surface Characterization

PETG sheets were first activated by glow discharge treatment, and then treated with 3-aminopropyltriethoxysilane (APTES) to introduce amino groups on the surface. Poly(GMA-*co*-SBMA) copolymers or GMA monomers were then grafted on the surface by the one-step ring-opening reaction of the epoxy groups and amino groups under alkaline condition to obtain G-*co*-S-coated

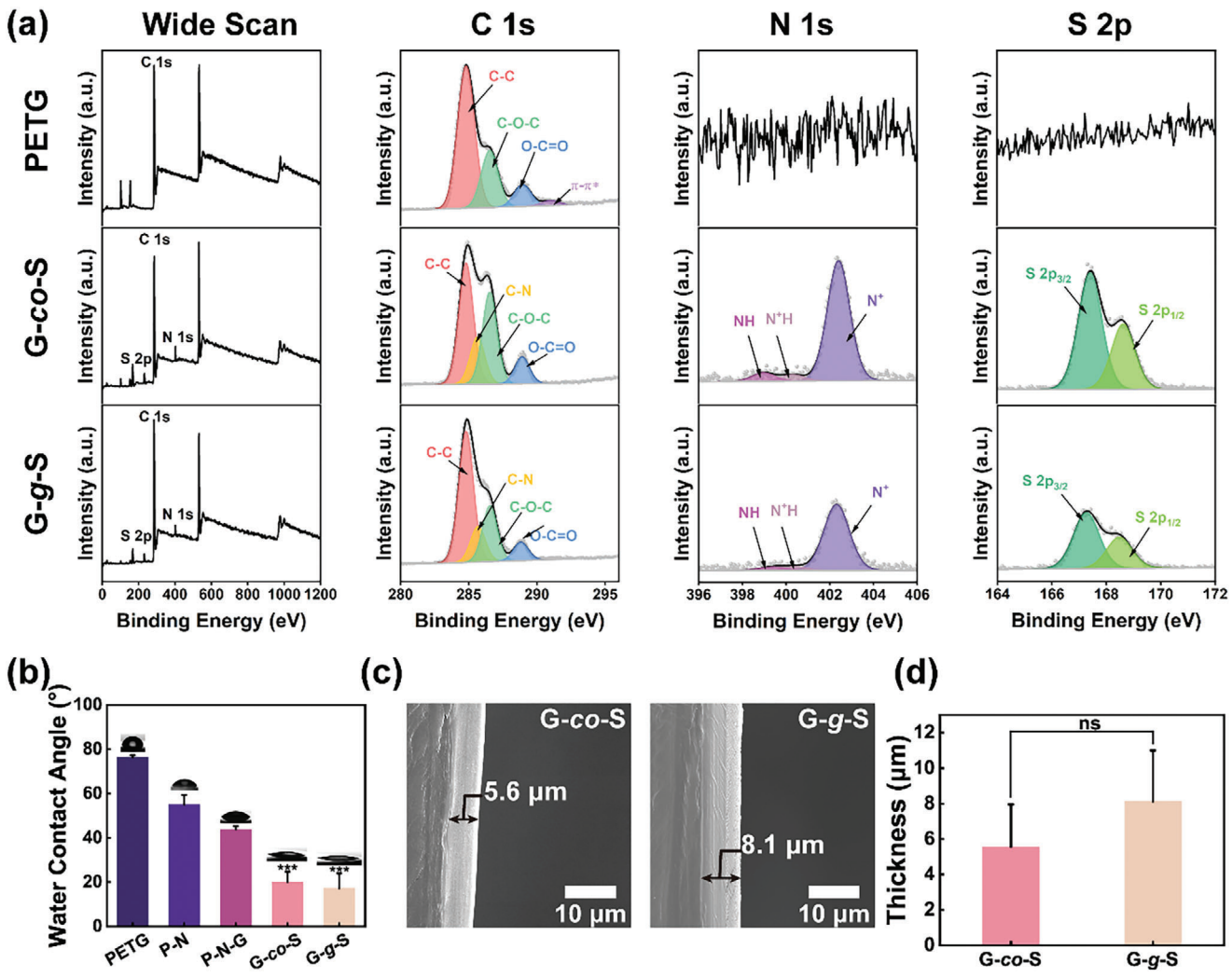

Figure 2. Surface characterization. a) XPS wide scan and C 1s, N 1s, and S 2p core-level spectra of pristine and coated PETG surfaces. b) Water contact angle of PETG sheets before and after coating, *** indicates $p < 0.001$ compared with PETG. c) SEM cross-section and d) coating thickness of G-*co*-S coating and G-*g*-S coating on PETG sheet.

surface or GMA-functionalized surface (Scheme 1). For the GMA-functionalized sheet, it was then immersed in an SBMA solution and proceeded with a free radical polymerization reaction to obtain a G-*g*-S coating. The PETG sheets before and after various coating steps were analyzed using X-ray photoelectron spectroscopy (XPS) (**Figure** 2a). A characteristic peak of C—N at ≈285.6 eV, as well as signal peaks of N 1s and S 2p appeared on the G-*co*-S- and G-*g*-S-coated PETG sheets, indicating the successful G-*co*-S and G-*g*-S coatings on PETG sheets.

The surface contact angle decreased from 76.5±0.8° of pristine PETG to 55.1±4.2° of aminated PETG surface (P-N surface), and further decreased to 43.8±1.5° of GMA-grafted aminated PETG surface (P-N-G surface) (Figure 2b). The G-*co*-S and G-*g*-S coatings showed good hydrophilicity with contact angles of 20.1±4.7° and 17.2±6.7°, respectively. This is because that the introduction of zwitterionic polySBMA polymer chains on the surface increased the hydrophilicity. The cross-section of G-*co*-S and G-*g*-S coatings was observed using scanning electron microscopy (SEM) (Figure 2c), and the thickness of the coating was determined to be 5.6 ± 2.4 μm of G-*co*-S coating and 8.1 ± 2.9 μm of G-*g*-S coating (Figure 2d). Although the G-*g*-S coating showed a slightly higher thickness compared to the G-*co*-S coating, there is no significant difference between the two groups.

Transparency is an important property for the aesthetic appearance of invisible aligners. The transmittance of pristine PETG, and G-*co*-S- and G-*g*-S-coated PETG sheets was around 90% at 400–800 nm (Figure S1, Supporting Information), and there was no variability between the three groups, indicating that the presence of the coating did not alter the transparency of PETG. In addition, mechanical properties of invisible aligners are crucial for orthodontic treatment as it controls tooth movement through deformation of the plastic.[28] The tensile strength and elastic modulus of the G-*co*-S- and G-*g*-S-coated PETG were almost unchanged compared to those of the pristine PETG (Figure S2, Supporting Information), confirming the process of surface modification does not alter the mechanical properties of PETG.

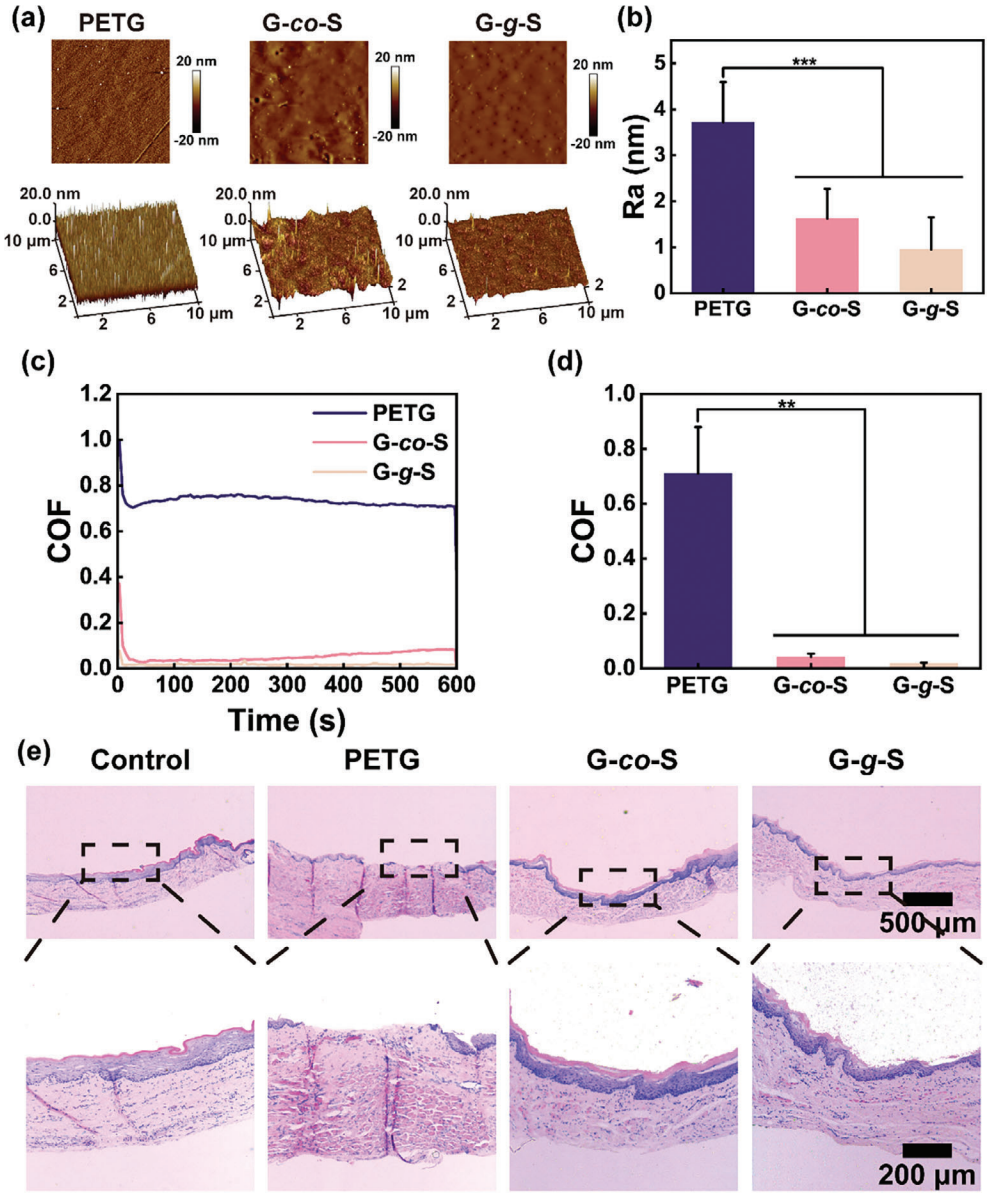

Figure 3. Surface roughness and lubricity. a) AFM 2D and 3D images of PETG, and G-*co*-S- and G-*g*-S-coated PETG surfaces. b) Ra value of PETG, and G-*co*-S- and G-*g*-S-coated PETG surfaces. c) Representative COF-time curve, and d) COF values between flat pristine PETG, and G-*co*-S- and G-*g*-S-coated surfaces and PDMS ball. No significant difference was detected between G-*co*-S and G-*g*-S surfaces. e) Representative images of H&E of rat oral mucosa after the friction test rubbed with different PETG surfaces.

2.3. Surface Roughness and Lubricity

Subsequently, surface morphology of PETG, G-*co*-S, and G-*g*-S sheets was analyzed using atomic force microscopy (AFM) (**Figure** 3a). It could be observed that G-*co*-S and G-*g*-S coatings significantly improved the surface smoothness, and the Ra values decreased from 3.72 ± 0.87 nm of pristine PETG sheet to 1.62 ± 0.64 nm of G-*co*-S sheet, and 0.95 ± 0.70 nm of G-*g*-S sheet (Figure 3b). Although the G-*g*-S sheet seems to have a smoother surface compared to the G-*co*-S sheet, there is no significant difference between the two groups. It is generally accepted that a smooth coating is beneficial for inhibiting fouling on the surface as well as reducing abrasion on the surrounding mucosal tissues.[29]

The uneven surface of aligners will constantly rub the oral mucosa, while they are being worn, which may consequently lead to oral ulcers. One of the approaches to reduce the friction between the aligner surface and oral mucosa is to modify the surface with a lubricious coating. Herein, the friction of the PETG surface after coating was investigated. First, saline was used as a lubricant to simulate the liquid environment in the oral cavity, and polydimethylsiloxane (PDMS) material was used as the friction head, and the coefficient of friction (COF) between the friction pair (i.e., PDMS ball and flat PETG surface with or

without coating) was obtained via a linear reciprocating motion as reported previously[30] (Figure S3, Supporting Information). As can be seen, the COF values of the G-*co*-S- and G-*g*-S-coated PETG surfaces were much smaller than that of the uncoated PETG surface, and the low COF of the G-*co*-S and G-*g*-S coatings could be maintained stably over the test period (Figure 3c). The COF of the uncoated PETG sheet was 0.711 ± 0.168. After coating with G-*co*-S and G-*g*-S, it decreased to 0.043 ± 0.011 and 0.018 ± 0.003, respectively (Figure 3d). The coating's ability to form a hydrated layer on its surface in a liquid environment can significantly reduce the surface friction properties, thereby enhancing its lubrication performance.

To further investigate the frictional effect of the coatings on oral mucosa, PETG sheet was hammered using a stainless-steel ball into a shape with a curved surface, modified with G-*co*-S or G-*g*-S coating, and used as the frictional head. Oral mucosa from rats was fixed on a flat Ti6Al4V sheet to form the frictional pair (Figure S3, Supporting Information). Linear reciprocating abrasion was performed on the mucosa for 1 min (total travelling distance: 4 mm). The SEM images showed that, compared to the control group (mucosa without abrasion), the mucosa rubbed by the pristine PETG surface showed obvious signs of rupture, while the mucosa of the G-*co*-S and G-*g*-S groups showed little signs of rupture (Figure S4, Supporting Information). The hematoxylin & eosin (H&E) staining images also confirmed that the mucosal layer was destructed after abrasion with PETG, while it remained relatively intact after abrasion with the G-*co*-S- and G-*g*-S-coated surfaces (Figure 3e). The outcomes of the mucosal abrasion test demonstrated that the lubricating properties of G-*co*-S and G-*g*-S coatings are beneficial in reducing intraoral friction and protecting the oral mucosa when using aligners.

2.4. Coating Stability

To get optimal orthodontic results, it is advised that patients wear invisible aligners for more than 20 h a day and replace them every 1–2 weeks.[2,10,31,32] The coatings on the surface of the aligners need to be stable and maintain their functionality over an extended period of exposure to the complex oral environment. The G-*co*-S- and G-*g*-S-coated sheets were first stored in air and in artificial saliva for up to 2 weeks, and the surface characteristics and frictional properties of the coating were then investigated. From the XPS results, the N 1s and S 2p signals remained obvious on the G-*co*-S and the G-*g*-S surfaces both in air and in artificial saliva for 2 weeks (**Figure** 4a,b). The N/C ratio of the coatings slightly increased after prolonged incubation (Table S1, Supporting Information). This could be attributed to the residual NH_4^+ ions from the artificial saliva onto surface. The change in water contact angle of pristine PETG sheet and PETG with G-*co*-S and G-*g*-S coatings after incubation in artificial saliva for up to 14 days was recorded (Figure 4c). The contact angle of pristine PETG surface remained at around 70.0° over the tested period. After 1 day of incubation, the contact angles of G-*co*-S and G-*g*-S increased to 42.4 ± 3.9° and 37.2 ± 2.3°, respectively. But they did not change dramatically afterward and remained below 50° over 14 days. The XPS and water contact angle results showed that both the G-*co*-S and G-*g*-S coatings have good stability.

The friction properties of the substrates after soaking in artificial saliva for 14 days was further investigated (Figure 4d). The COF value pristine PETG was 0.499 ± 0.082, which is lower than that of PETG sheet before soaking (0.711 ± 0.168, Figure 3d). This is probably because of residual components of artificial saliva, which is used to lubricate the oral mucosa to a certain extent[33] The COF values of G-*co*-S coating and G-*g*-S coating were 0.045 ± 0.025 and the 0.062 ± 0.014, respectively, which were slightly increased compared to those before soaking (0.043 ± 0.011 and 0.018 ± 0.003, Figure 3d), but still significantly lower than the pristine PETG. This suggests that both coatings can effectively maintain their lubricating properties in a simulated oral environment for an extended period.

It should be noted that the coating thickness decreased, and some porous structure was observed in the coating layer after incubation in artificial saliva for 14 days (Figure S5, Supporting Information), possibly due to release of the noncovalent (i.e., electrostatic interactions, hydrogen bonding, and molecular chain entanglements, etc.) bonded polymer segments from the coatings or degradation of the polymer chains during incubation. Nevertheless, the above results demonstrate that the G-*co*-S and G-*g*-S coatings have good stability on the surface in a simulated oral environment and have well preserved their lubricity over prolonged time, which are promising for aligner applications.

2.5. Antifouling and Antiadhesive Properties

Oral environment is complicated as it containing a lot of proteins and other biomolecules, which could attached to the aligner surface quickly and create sites for bacterial adhesion.[5] Antifouling performance of the aligner surface is important for reducing protein adsorption and sebsueqent bacterial adhesion. PETG sheets before and after coating were incubated in fluorescein isothiocyanate (FITC)-lableled bovine serum protein (BSA) solution to evaluate its antifouling performance. As can be seen, green fluorescence signal was observed on the surface of pristine PETG (Figure S6, Supporting Information). In contrast, the G-*co*-S and G-*g*-S coatings showed low green fluorescence signal on their surfaces. The overall fluorescence intensity decreased by 76% and 81% after G-*co*-S and G-*g*-S coatings, respectively (**Figure** 5a), demonstrating antifouling effects of the coatings. As mentioned above, some polymer chains might release from the coatings due to noncovalent bonding or degradation slowly (Figure S5, Supporting Information), and this could also contribute to the antifouling performance of the surfaces.

Over time, bacteria wound accumulate and form plaque on the aligner surface, which increases the risk of dental caries and other oral diseases.[34–36] *S. mutans* is the primary causative agent of dental caries and aids in the initial colonization of other bacteria that can cause dental caries by producing extracellular polymeric substances and acids, leading to the formation of early dental plaque.[34] *Staphylococcus aureus* (*S. aureus*) and *Escherichia coli* (*E. coli*) are common causative agents and major causes of hospital- and community-acquired infections.[37] They attach to medical implants and host tissues and play an important role in the persistence of chronic infections.[38] In this study, the antimicrobial properties of the coatings against Gram positive *S. mutans* and *S. aureus*, and Gram negative *E. coli* were investigated.

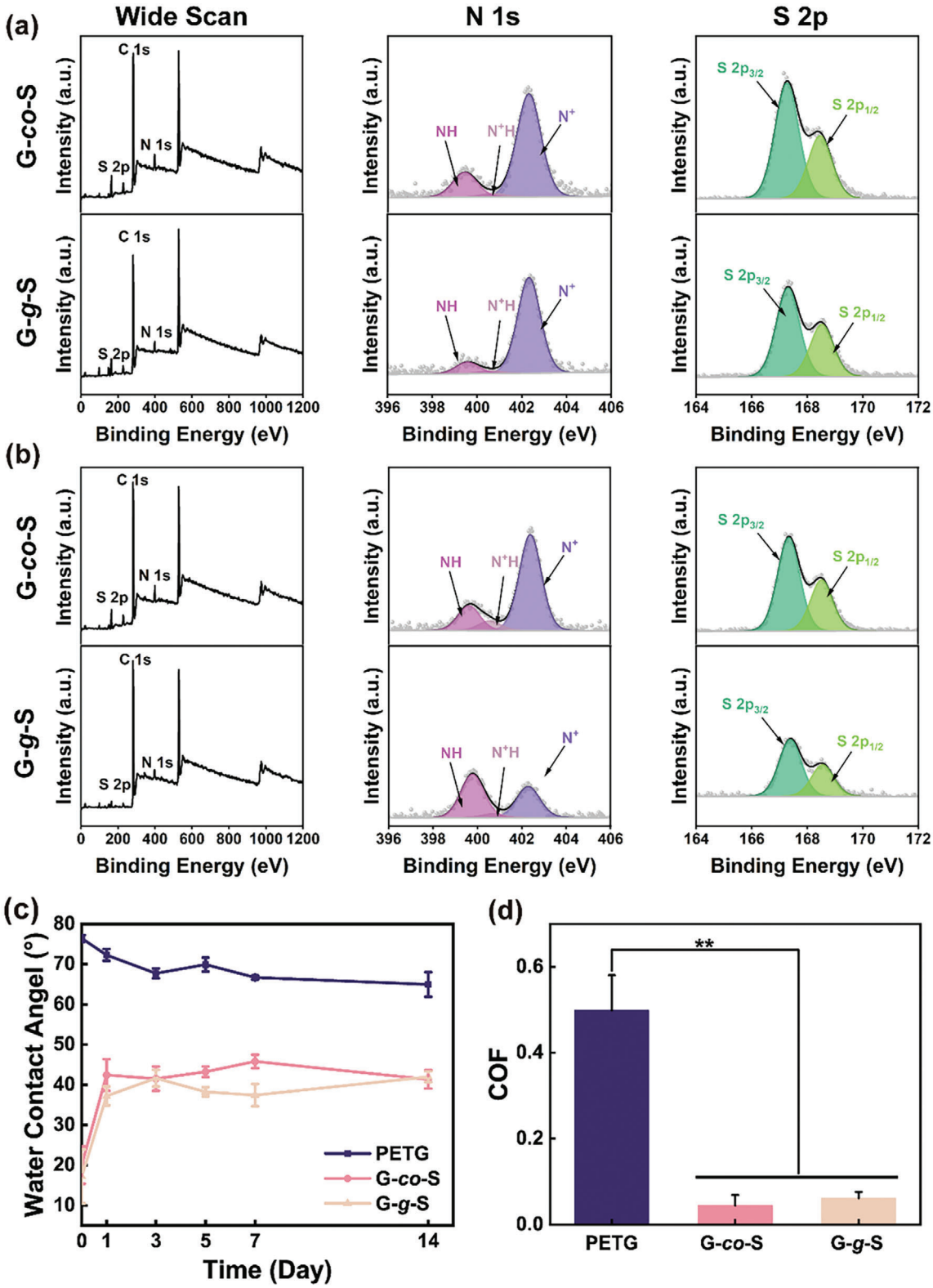

Figure 4. Coating stability. XPS wide scan and N 1s and S 2p core-level spectra of G-*co*-S and G-*g*-S coatings after storage in a) air and b) artificial saliva for 14 days. c) Changes in water contact angle of pristine PETG surface and G-*co*-S- and G-*g*-S-coated surfaces after incubation in artificial saliva for different periods of time. d) COF of pristine PETG surface and G-*co*-S- and G-*g*-S-coated surfaces after incubation in artificial saliva for 14 days.

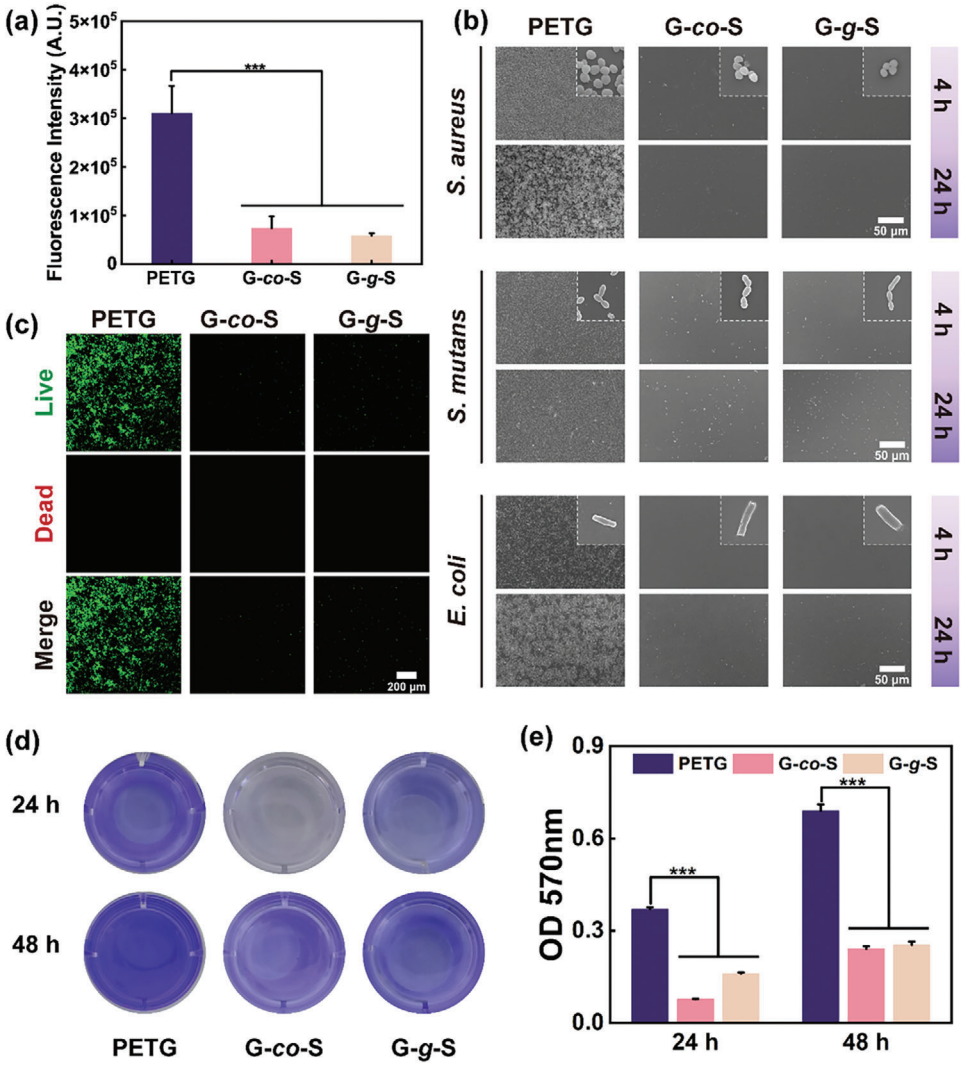

Figure 5. Antifouling and antibacterial abilities of aligners before and after coating. a) Quantitative results of fluorescent intensity of PETG surfaces before and after coating incubated in 4 mg mL^{-1} of FITC-labeled BSA for 1 h. b) SEM images of PETG surfaces before and after coating incubated in bacterial suspension (10^8 cells mL^{-1} in PBS) for 4 and 24 h. c) Representative fluorescent images of *S. aureus* adhesion on different PETG surfaces after incubation in bacterial suspension (10^8 cells mL^{-1} in PBS) for 24 h. d) Representative photographs and e) quantitative results of *S. aureus* biofilms formation on different PETG surfaces after incubation in bacterial suspension (10^6 cells mL^{-1} in culture medium) for 24 and 48 h and stained with crystal violet.

Pristine PETG sheet and G-*co*-S- and G-*g*-S-coated PETG sheets were first submerged in a phosphate-buffered saline (PBS) suspension containing 10^8 cells mL^{-1} of bacteria to investigate their capability against bacterial adhesion. After 4 h of immersion, a large number of bacteria adhered to the pristine PETG sheet (Figure 5b). In contrast, the bacterial adherence to the G-*co*-S and G-*g*-S sheets was obviously inhibited. After 24 h, the number of bacteria adhering to the G-*co*-S and G-*g*-S sheet surfaces was still low, which was quite different from that on the pristine PETG sheet. The live/dead staining showed a similar trend of much lower number of adhering bacteria on the G-*co*-S and G-*g*-S surfaces (Figure 5c). These findings indicate that the G-*co*-S and G-*g*-S coatings actively impeded the initial attachment of bacteria.

To further evaluate the inhibitory capability of the coatings against biofilm formation, the samples were incubated with *S. aureus* in culture medium for 1 and 2 days. The amount of biofilm was semiquantified by crystal violet staining (Figure 5d,e). As can be seen, after 1 day of incubation, the optical density (OD) values of G-*co*-S and G-*g*-S groups were 0.08 and 0.16, respectively, while that of PETG group was 0.37. Both G-*co*-S and G-*g*-S coatings exhibited significantly lower amounts of biofilm formation compared to PETG, indicating the biofilm resistance properties of G-*co*-S and G-*g*-S coatings. After two days, the G-*co*-S and G-*g*-S coatings still exhibited significant inhibitory effects. This indicates that the coatings have a sustainable resistance to biofilm. The zwitterionic groups in the G-*co*-S and G-*g*-S coatings have a strong ion-solubilizing effect, and they can firmly and stably bind water molecules through hydrogen bonding, forming a hydrated barrier to reduce protein adsorption as well as bacterial adhesion.[39]

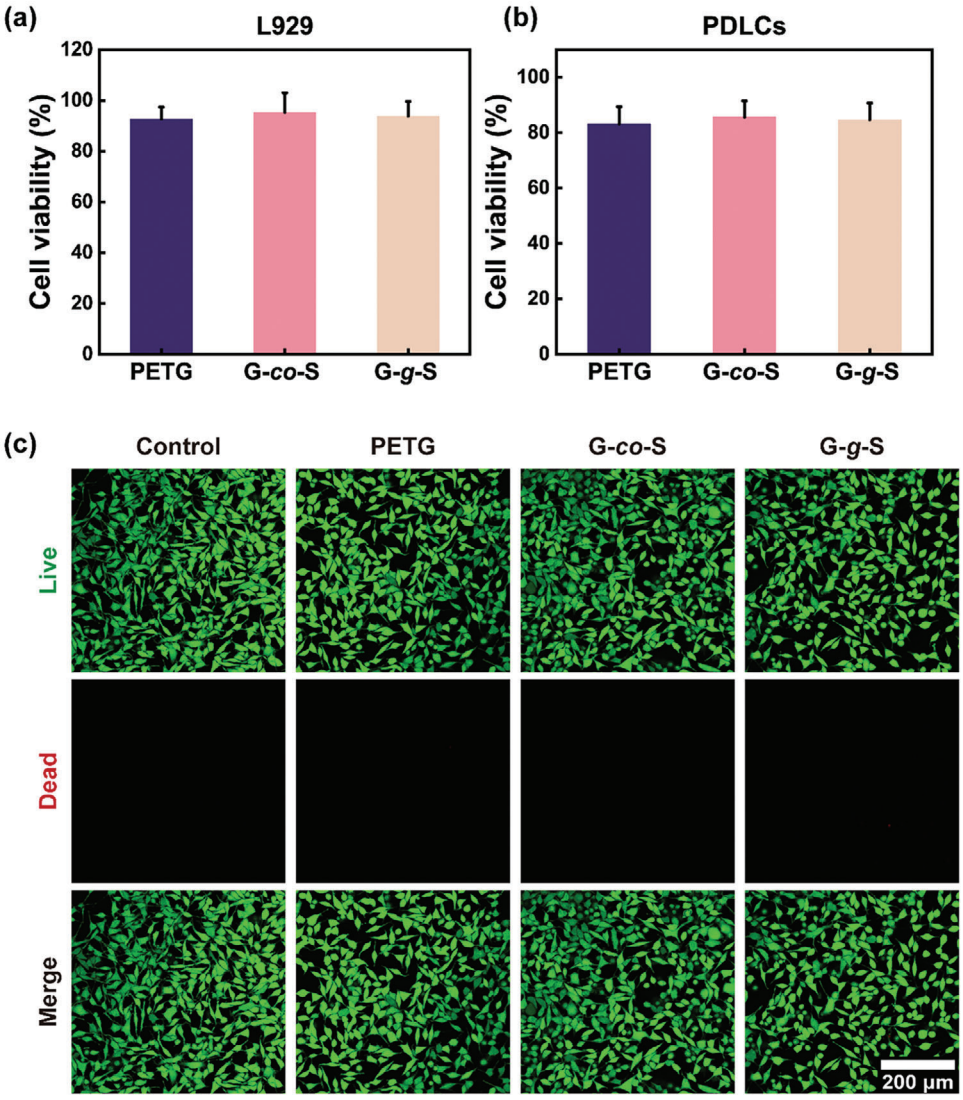

Figure 6. In vitro biocompatibility. Cell viability of a) mouse fibroblasts (L929) and b) periodontal cells (PDLCs) after incubation with extract of PETG, and G-*co*-S- and G-*g*-S-coated PETG sheets for 24 h. c) Fluorescence images of L929 cells after incubation with the extract medium for 24 h.

2.6. In Vitro Biocompatibility

Optimal biocompatibility is essential for antimicrobial coatings on biomedical devices like aligners. This study investigated the potential cytotoxic effect of the coatings on mouse fibroblast L929 cells and human periodontal cells (PDLCs). We cultured these cells in the extract medium of the pristine and coated PETG sheets, and the possible cytotoxic effect was assessed using the Cell Counting Kit-8 (CCK-8) assay. After 24 h culture, the survival ratios of both types of cells were over 80% in all groups (**Figure** 6a,b). The morphology and viability of the cells were assessed using live/dead staining. After 24 h culture, L929 cells cultured with the extracts of pristine PETG, and G-*co*-S- and G-*g*-S-coated PETG were all green in color and exhibited the appearance of typical stellate or spindle-forming fibroblasts, with no cell death, cytolysis, and inhibition of cell growth were observed (Figure 6c). These results indicated that the G-*co*-S and G-*g*-S coatings have negligible cytotoxicity in vitro and maintain good biocompatibility.

2.7. In Vivo Oral Mucosa Irritation

Because the aligner would come into direct contact with the oral mucosa during orthodontic therapy, the in vivo compatibility of the coated material is significantly important. To investigate the possible irritation effect of the coatings on oral mucosa, the G-*co*-S- and G-*g*-S-coated PETG sheets were implanted in the oral cavity of rats for 14 days (**Figure** 7a). After implantation, the oral mucosa tissues in contact with the pristine PETG sheets, G-*co*-S- and G-*g*-S-coated PETG sheets were collected to analyze for possible inflammatory reaction and compared with the blank group (without any treatment) and the sham group (sew up the mucosa without sheets). The H&E staining results showed that the oral

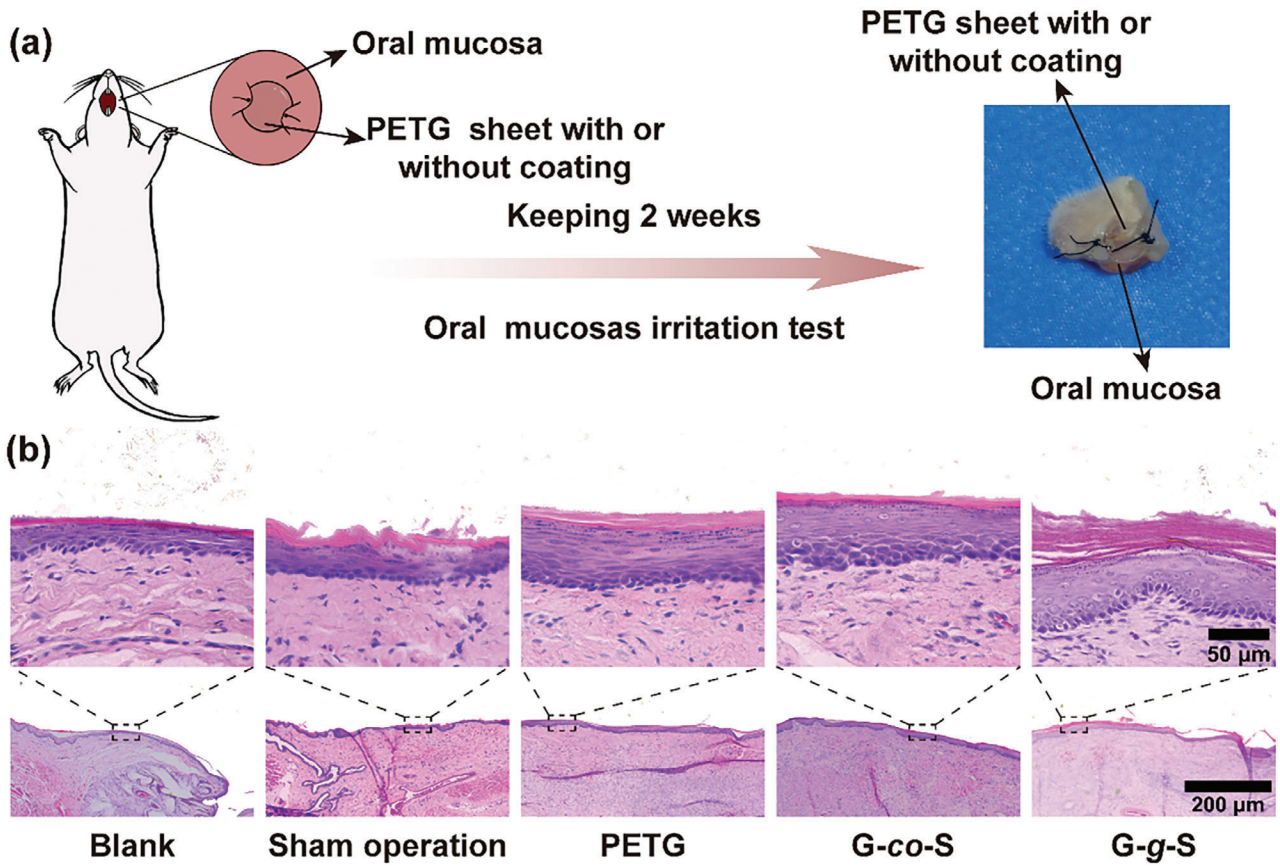

Figure 7. Oral mucosa irritation test. a) Schematic diagram of oral mucosa irritation test in rats. b) Representative images of H&E staining of rat oral mucosa of the blank and sham groups, and groups of mucosa in contact with pristine PETG, and G-*co*-S-coated and G-*g*-S-coated PETG sheets for 14 days.

mucosa in the experimental groups (i.e., PETG, G-*co*-S, and G-*g*-S groups) were the same as the blank group and the sham group, with a uniform thickness of the intact mucosal layer, and no buccal/lingual mucosal lesions, significant inflammation, or other lesions were observed (Figure 7b). This further confirmed that the presence of G-*co*-S coating and G-*g*-S coating on the aligner did not cause irritation to the oral mucosa, and it could be safely used in the oral cavity for prolonged time.

3. Conclusion

In summary, this study has successfully developed polyzwitterionic coatings with good lubricating and antibacterial properties on invisible aligner materials. The coatings were prepared by directly grafting poly(GMA-*co*-SBMA) to the APTES-aminated PETG surface (i.e., G-*co*-S surface), or by grafting polySBMA via free radical polymerization on the GMA-factionalized PETG surface (i.e., G-*g*-S surface). The coatings formed a hydration layer on the substrate surface, which significantly improved the hydrophilicity of the surface and reduced the surface friction coefficient, while did not affecting the transparency and mechanical properties of the PETG sheets. The linear reciprocating friction test with rat oral mucosa confirmed that the wear effect on the mucosa by PETG substrates was significantly reduced after G-*co*-S and G-*g*-S coatings. The G-*co*-S and G-*g*-S coatings could reduce protein adsorption and bacterial adhesion, and inhibit biofilm formation on the surface significantly, which is promising to suppress the formation of dental plaque on invisible aligners. The G-*co*-S and G-*g*-S coatings also exhibited good stability when stored in air and in a moist environment that simulates the oral cavity. The in vitro cell experiments and in vivo animal experiments demonstrated that the coated PETG substrates exhibited excellent biocompatibility and did not cause any irritation to the oral mucosa. There is no discernible difference in the antibacterial performance, lubricating functions, or biocompatibility of the G-*co*-S and G-*g*-S coatings constructed through the "grafting to" and "grafting from" approaches. However, considering the feasibility of the coating process, G-*co*-S coating would have more development prospects in clinical applications. This study provided facile approaches for development of biocompatible coatings with significant benefits in reducing surface friction and inhibiting bacterial adhesion and biofilm formation, which are promising for aligner applications.

4. Experimental Section

Materials: Glycidyl methacrylate (GMA) was purchased from Sigma-Aldrich (Shanghai, China). [2-(Methacryloyloxy)ethyl]dimethyl-(3-sulphonatopropyl)ammonium hydroxide (SBMA), 3-aminopropyltriethoxysilane (APTES), poly(ethylene glycol) diacrylate (PEGDA, molecular

weight: 600 Da), and 2-hydroxy-2-methylphenylpropanone (Irgacure 1173) were purchased from Aladdin (Shanghai, China). Triethylamine (TEA) was purchased from Energy Chemical (Shanghai, China), Azobisisobutyronitrile (AIBN) was purchased from Shanghai Shisihewei Chemical (Shanghai, China). Biolon polyethylene terephthalate glycol (PETG) sheets (Φ 120, δ 0.75 mm) were obtained from Dreve Dentamid GmbH (Belgium, Germany). Bovine serum protein (BSA) and fluorescein isothiocyanate (FITC) were purchased from Macklin (Shanghai, China). Mouse fibroblasts (L929) were purchased from Nation Collection of Authenticated Cell Cultures (Shanghai, China). Human periodontal cells (PDLCs) were obtained from West China Hospital of Stomatology, Sichuan University (Sichuan, China). *Staphylococcus aureus* (*S. aureus*) ATCC 6538 and *Escherichia coli* (*E. coli*) ATCC 11 229 were purchased from China General Microbial Culture Collection Center (Beijing, China). *Streptococcus mutans* (*S. mutans*) BNCC 186 308 was purchased from BeNa Culture Collection (Henan, China). Artificial saliva, Tryptic Soy Broth (TSB), and Lysogeny Broth (LB) were obtained from Solarbio (Beijing, China). Brain Heart Infusion Broth (BHI) was obtained from Beijing Land Bridge Technology (Beijing, China).

Synthesis of Poly(GMA-co-SBMA): First, 9.21 g SBMA (32 mmol) and 1.17 g GMA (8 mmol) were added into 80 mL methanol/acetonitrile mixture (equal volume) to form a solution with the total monomer concentration of 0.5 M. The solution was stirred for 10 min, and then purged with nitrogen for 15 min. After that, 0.064 g of AIBN (1% of the total monomer) was added to the solution, and followed by mixing for another 15 min. The solution then proceeded to reaction at 70 °C for 6 h. The product was purified by ethanol three times at the end of the reaction. The final precipitate was dissolved in deionized water and lyophilized to obtain white powder of poly(GMA-*co*-SBMA) polymer.

Characterization of Poly(GMA-co-SBMA): The polymers were characterized using Gel Permeation Chromatography (GPC, PL-GPC50, Agilent, USA, a PL aquagel-OH column was used with 0.1 M $NaNO_3$ as the mobile phase at a flow rate of 1.0 mL min^{-1}), FT-IR (Thermo Fisher, IS 50, USA) in attenuated total reflection model, and ^{1}H NMR (Bruker, AVANCE NEO 400 MHz, with deuterate water as the solvent).

To determine the epoxy value of poly(GMA-*co*-SBMA), 0.5 g of the polymer was added in 20 mL of hydrochloric acid – acetone mixture (volume ratio of concentrated hydrochloric acid to acetone = 1: 40) in a conical flask. It was covered with aluminum foil to keep away from light and shaken thoroughly to completely dissolve the polymer. After that, the solution was incubated statically for 30 min, and ≈2–3 drops of 0.1% methyl red indicator were added. The polymer solution was titrated using 0.1 mol L^{-1} sodium hydroxide solution until it turned from red to yellow and the color remained unchanged within 30 s. The volume of sodium hydroxide solution consumed was recorded, and the same amount of polySBMA (prepared in the same method as described above with 32 mmol of SBMA) was used as the control. The epoxy value of the polymer (Ev, equivalent each 100 g sample) was calculated according to the equation below

$$Ev = \frac{(V_0 - V_1)\, N}{1000W} \times 100 \quad (1)$$

whereas V_0 is the volume of sodium hydroxide solution (mL) consumed for the blank titration, V_1 is the volume of sodium hydroxide solution consumed for the sample titration, N is concentration of sodium hydroxide solution (0.1 mol L^{-1}), and W is the mass of the sample tested (0.5 g).

Preparation of Coatings on PETG via "Grafting to" and "Grafting from" Methods: PETG sheet (cut into size of Φ 10 mm, except 15 mm × 30 mm × 0.75 mm for the friction test, Φ 16 mm for the cytotoxicity test, or 9 mm × 50 mm dumbbell-shaped specimen for the tensile strength test) was soaked in isopropyl alcohol for 10 min, followed by sonication in deionized water for 40 min in an ice-water bath. After sonication, the PETG sheet was rinsed with deionized water and blown dry with N_2. The dried PETG sheet was treated with glow discharge treatment at 15 mA for 2 min (Glow Discharge Cleaning System, easiGlow 91 000, PELCO, USA) to improve the surface hydrophilicity. Subsequently, the PETG sheet was immersed in 2 mL (5 mL for the friction test sample, 3 mL for the cytotoxicity test sample, or 8 mL for the tensile strength test sample) of APTES solution (1 mM in anhydrous ethanol) at room temperature overnight. After that, it was rinsed with deionized water and dried with N_2. The aminated substrates were named as P-N, and then coated through two different methods as described below.

"Grafting to" method: The aminated substrate was immersed in appropriate volume of aqueous solution containing 7 mg mL^{-1} of poly(GMA-*co*-SBMA) and 10 µL mL^{-1} of TEA for 6 h in a water bath at 37 °C. After that, the unbounded poly(GMA-*co*-SBMA) was removed by rinsing with deionized water and the substrate was dried in a N_2 flow. The sample prepared via the "grafting to" method was denoted as G-*co*-S.

"Grafting from" method: The aminated substrate was immersed in appropriate volume of methanol solution containing 13.7 µL mL^{-1} of GMA and 10 µL mL^{-1} of TEA. The reaction was carried out in a water bath at 37 °C for 6 h to obtain GMA-grafted sheets, which were named P-N-G. The unbounded GMA monomer was removed by rinsing with deionized water, and the substrate was dried in a N_2 flow. The P-N-G sheet was then immersed in appropriate volume of aqueous solution containing 0.115 g mL^{-1} of SBMA, 6.3 µL mL^{-1} of PEGDA (0.3% of the total monomer), and 6 µL mL^{-1} of Irgacure 1173 (1% of the total monomer), and irradiated under 365 nm ultraviolet light for 30 min. The collected substrate was then rinsed with copious amounts of deionized water and dried in a N_2 flow. The sample prepared via the "grafting from" method was denoted as G-*g*-S.

Coating Characterization: Surface hydrophilicity of the PETG sheets before and after coating was measured using a contact angle goniometer (KRUSS, DSA25E, Germany) via the sessile drop method with 1 µL of deionized water dropped on the sample surface at room temperature. The contact angle was measured after 10 s. Five different positions on the surface of the samples were randomly measured. The chemical composition of the surfaces was determined by XPS (Kratos, Axis Ultra DLD, UK). The binding energy of C 1s was calibrated to 284.8 eV as the reference. The various element ratios on the coating were calculated using CasaXPS (Version 2.3.25PR1.0). The surface roughness of PETG sheets was characterized using an AFM (Bruker, Fast Scan, USA). The microstructure of the sample surface was captured with Scan Asyst mode in air using a scanasyst-air probe at 0.999 Hz scan rate. The PETG sheets after coating were immersed in liquid nitrogen, fractured to obtain the cross-section for observation of the coating thickness using SEM (S4800, Hitachi, Japan). The transmittance of the PETG samples before and after coating was scanned at 200–800 nm using a UV–Vis–NIR spectrophotometer (Cary 5000, Agilent, USA). For the tensile properties, PETG samples were cut into 9 mm × 50 mm dumbbell-type specimens and tested using a universal testing machine (CMT-1104, SUST, China) at a crosshead speed of 1 mm min^{-1} until 7% tensile strain.

Tribological Test: Tribological properties of the samples were tested through a pin-on-plate tribometer (Bruker, UMT-TriboLab, USA). All PETG sheets (15 mm × 30 mm × 0.75 mm) with or without coating were subjected to 10 min of linear reciprocating friction at 10 mm s^{-1} using a 6 mm PDMS ball with a load of 2 N and a stroke of 10 mm at room temperature, with physiological saline as the lubricant. The COF was calculated by the data processing software of the UMT TriboLab (Data Viewer, Version 2.22.115. Build 2). The abrasion effect of the coating on mucous membrane was conducted in a similar manner as described above, except that rat oral mucosa was fixed onto the flat Ti6Al4V sheet, and a PETG hemisphere (Φ 7 mm, with or without coating, its curved surface was formed before the coating process by hammering using a 6.35 mm stainless steel ball) was fixed as the friction head. The period for linear reciprocal abrasion was set to 1 min at 4 mm s^{-1} with a load of 1 N and a stroke of 4 mm. The oral mucous membranes before and after abrasion were subjected to gradient dehydration and observed using SEM or stained with H&E (Solarbio, China) and observed using an inverted microscope (Leica, DMIL LED, Germany).

Coating Stability: To investigate the coating stability, PETG sheets were exposed in air at room temperature or incubated in artificial saliva at 37 °C with shaking for 14 days, and the surface elements, hydrophilicity and frictional properties of the sheets were analyzed using XPS, contact angle measurements, and friction test at predetermined times as described above.

Protein Adsorption: FITC-labeled BSA was prepared as reported in the literature[13] by slowly addition of 1 mL of FITC (9 mg mL^{-1} in methanol) to 100 mL of BSA solution (5 mg mL^{-1} in PBS, pH = 7.4), which was stirred in the dark at room temperature for 4 h. The solution was dialyzed with PBS and deionized water successively in the dark until the light absorbance value of the dialysate at 495 nm was below 0.003, and then lyophilized. One hundred and fifty microliters of FITC-labeled BSA solution (4 mg mL^{-1} in PBS) was dropped to cover the sample surface and incubated in the dark at 37 °C for 1 h. The surface was washed three times with PBS, and the proteins adsorbed on the surface of the samples were observed by confocal laser scanning microscopy (CLSM, Leica, TCS SP8, Germany). The fluorescent intensity on each surface was calculated using ImageJ software (Version 1.54 d).

Bacterial Adhesion and Biofilm Formation: *S. aureus*, *S. mutans*, and *E. coli* were cultured with TSB, BHI, and LB media, respectively, overnight in a shaker at 37 °C, harvested by centrifugation, and resuspended in PBS (10 mM, pH 7.4). The sheets (Φ 10 mm) were placed in a sterilized 24-well plate with each well containing 2 mL bacterial suspension (10^8 cells mL^{-1}). After incubation at 37 °C for 4 and 24 h, the sheets were washed with PBS three times to remove any unadhered bacteria, dehydrated and observed using SEM. The samples were incubated in *S. aureus* suspension for 24 h, stained with Live/Dead BacLight bacterial viability kit (Thermo Fisher Scientific, USA), and observed using CLSM. To investigate the long-term resistance of the coating to biofilms, *S. aureus* was diluted to 10^6 cells mL^{-1} with TSB containing 1% sucrose. PETG sheet was incubated in 2 mL bacterial solution for 24 and 48 h, with the medium being changed every 24 h. The amount of biofilm on the sheet surface was subsequently stained by crystal violet, dissolved using 33% acetic acid, and quantified by measuring the OD of the solution at 570 nm (the background OD value of the respective sample stained by crystal violet was subtracted).

In Vitro Cytotoxicity Assay: L929 fibroblasts and human periodontal cells (PLDCs) were cultured in Dulbecco's Modified Eagle's Medium (DMEM, Biosharp, Anhui, China) supplemented with 10% fetal bovine serum (FBS, Gibco, USA), 1% antibiotic solution (penicillin-streptomycin, Biosharp, Beijing, China), and 1% growth factor (MEM Non-Essential Amino Acids, Gibco, USA) at 37 °C in 5% v/v CO_2 atmosphere.

Any potential toxic substances were extract by incubating the sheets (Φ 16 mm) in 0.665 mL of the culture medium (the coating side was facing downside to ensure fully contacting the medium) in a 6-well plate for 24 h at 37 °C. The extract medium was filtered through a 0.22 μm sterile filter. For the quantification assay, cells were first seeded in 96-well plates at a density of 5×10^3 cells per well and incubated for 24 h. The culture medium was then replaced with the extract and the cells were incubated for another 24 h. After that, the cell viability was determined using the CCK-8 (Beyotime, Shanghai, China) assay according to the manufacturer's instructions. Medium without extract was used as a negative control and medium containing 1% Triton-X was used as a positive control. The experiment was repeated three times with five replicate wells for each group every time. The relative cell viability (%) was calculated by comparing the OD values of the experimental group with that of the control group. For the qualification assay, L929 fibroblasts were first inoculated in a 35 mm confocal dish at a density of 3×10^6 cells per dish and incubated for 24 h. The medium was then replaced with the extract and incubated for another 24 h. The cells were stained with Calcein AM/PI Cell Viability/Cytotoxicity Assay Kit (Beyotime, Shanghai, China) as per the manufacturer's instructions and viewed using CLSM.

In Vivo Oral Mucosa Irritation Test: Any possible irritation effect of the coated PETG sheet on oral mucosa was evaluated through a rat model (Sprague–Dawley rats, female, 100–120 g, 5–6 weeks). The animal experiments were approved by the Institutional Animal Ethical Committee of West China Hospital of Stomatology, Sichuan University (approval number: WCHSIRB-D-2023-161). PETG sheets were cut into disks with a diameter of 4 mm and two holes with a diameter of 0.5 mm were made near the perimeter. The edge was rounded off using sandpaper. The internal and external oral tissues of the animals were cleaned with iodophor. The pristine and coated PETG sheets were placed on the buccal mucosal surfaces of both sides of the rat's oral cavity (one side for the pristine sheet and the other side for the coated sheet). The sheet was sutured carefully through the cheeks with medical 5-0 sutures for closely fitting it with the mucosa but not compressing the mucosal tissue. The animals were normally fed for 14 days. After that, the mucosa and surrounding tissue contacting the sheets were collected, fixed in 10% formalin, sectioned, and subjected to H&E staining to observe any inflammation.

Statistical Analysis: Statistical analysis was performed using SPSS software (version 18.0) according to the one-way ANOVA method. Data were expressed as mean ± standard deviation ($n \geq 3$), and p-value < 0.05 was considered statistically significant.

Supporting Information

Supporting Information is available from the Wiley Online Library or from the author.

Acknowledgements

This work was supported by Youth Innovation Promotion Association CAS (No. 2021296), Key Research and Development Program of Ningbo (No. 2022Z132), Foundation of Director of Ningbo Institute of Materials Technology and Engineering CAS (No. 2021SZKY0301), and Sichuan Science and Technology Program (No. 2023NSFSC1521).

Conflict of Interest

The authors declare no conflict of interest.

Author Contributions

R.W.: Conceptualization, Data curation, Investigation, Methodology, Writing — original draft. J.D.: Data curation, Methodology. X.G.: Methodology. Y.Y.: Methodology. J.M.: Methodology. A.L.: Methodology. H.C.: Methodology. X.H.: Methodology. Z.Z.: Conceptualization. X.C.: Conceptualization, Methodology, Supervision, Writing — review & editing. R.W.: Conceptualization, Methodology, Funding acquisition, Resources, Supervision, Writing — review & editing.

Data Availability Statement

The data that support the findings of this study are available from the corresponding author upon reasonable request.

Keywords

antiadhesive, antifouling, invisible aligner, lubrication, zwitterionic coating

Received: April 14, 2024
Revised: May 23, 2024
Published online:

[1] Y. M. Bichu, A. Alwafi, X. Liu, J. Andrews, B. Ludwig, A. Y. Bichu, B. Zou, *Bioact. Mater.* **2023**, *22*, 384.
[2] A. Papadimitriou, S. Mousoulea, N. Gkantidis, D. Kloukos, *Prog. Orthod.* **2018**, *19*, 37.
[3] C. Jordan, D. J. LeBlanc, *Oral Microbiol. Immunol.* **2002**, *17*, 65.
[4] N. Wang, J. Yu, J. Yan, F. Hua, *Front. Bioeng. Biotechnol.* **2023**, *11*, 1093926.

[5] Q. Xin, Z. Ma, S. Sun, H. Zhang, Y. Zhang, L. Zuo, Y. Yang, J. Xie, C. Ding, J. Li, *ACS Appl. Mater. Interfaces* **2023**, *15*, 41403.
[6] N. B. Pitts, D. T. Zero, P. D. Marsh, K. Ekstrand, J. A. Weintraub, F. Ramos-Gomez, J. Tagami, S. Twetman, G. Tsakos, A. D. C. Ismail, *Nat. Rev. Dis. Primers* **2017**, *3*, 17030.
[7] S. A. Ali, H. R. I. Miethke, *Dent. Update* **2012**, *39*, 254.
[8] V. Allareddy, R. Nalliah, M. K. Lee, S. Rampa, V. Allareddy, *Am. J. Orthod. Dentofacial Orthop.* **2017**, *152*, 706.
[9] M. Zhang, X. Liu, Y. Xie, Q. Zhang, W. Zhang, X. Jiang, J. Lin, *ACS Omega* **2020**, *5*, 18685.
[10] Y. Xie, M. Zhang, W. Zhang, X. Liu, W. Zheng, X. Jiang, *ACS Biomater. Sci. Eng.* **2020**, *6*, 1239.
[11] Y. Xie, W. Zheng, X. Jiang, *ACS Appl. Mater. Interfaces* **2020**, *12*, 9041.
[12] S. Park, H.-J. Jeong, J.-H. Moon, E.-Y. Jang, S. Jung, M. Choi, W. Choi, K. Park, H.-W. Ahn, J. Hong, *Appl. Surf. Sci.* **2022**, *578*, 152085.
[13] F. Sun, W. Hu, Y. Zhao, Y. Li, X. Xu, Y. Li, H. Zhang, J. Luo, B. Guo, C. Ding, J. Li, *Colloids Surf., B* **2022**, *217*, 112696.
[14] S. Park, H. Kim, S. B. Yang, J.-H. Moon, H.-W. Ahn, J. A. Hong, *ACS Appl. Mater. Interfaces* **2018**, *10*, 17714.
[15] Y. Zhang, W. Jiang, L. Lei, Y. Wang, R. Xu, L. Qin, Q. Wei, *Langmuir* **2022**, *38*, 7157.
[16] Y.-H. Huang, M.-J. Wang, T.-S. Chung, *Desalination* **2023**, *555*, 116527.
[17] S. Samanta, S. Sarkar, N. K. Singha, *ACS Appl. Mater. Interfaces* **2023**, *15*, 24812.
[18] A. B. Asha, Y. Chen, R. Narain, *Chem. Soc. Rev.* **2021**, *50*, 11668.
[19] J. Yang, H. Qian, J. Wang, P. Ju, Y. Lou, G. Li, D. Zhang, *J. Mater. Sci. Technol.* **2021**, *89*, 233.
[20] J. Miao, X. Wu, Y. Fang, M. Zeng, Z. Huang, M. Ouyang, R. Wang, *J. Mater. Chem. B* **2023**, *11*, 3373.
[21] Y. Yu, H. Yuk, G. A. Parada, Y. Wu, X. Liu, C. S. Nabzdyk, K. Youcef-Toumi, J. Zang, X. Zhao, *Adv. Mater.* **2019**, *31*, 1807101.
[22] J. Zhang, M. Wu, P. Peng, J. Liu, J. Lu, S. Qian, J. Feng, *ACS Appl. Mater. Interfaces* **2022**, *14*, 56097.
[23] S. Arango, A. Peláez-Vargas, C. García, *Coatings* **2013**, *3*, 1.
[24] K. Choy, *Prog. Mater. Sci.* **2003**, *48*, 57.
[25] Y.-N. Chou, T.-C. Wen, Y. Chang, *Acta Biomater.* **2016**, *40*, 78.
[26] S.-H. Tang, M. Y. Domino, A. Venault, H.-T. Lin, C. Hsieh, A. Higuchi, A. Chinnathambi, S. A. Alharbi, L. L. Tayo, Y. Chang, *Langmuir* **2019**, *35*, 1727.
[27] S. Mao, D. Zhang, Y. Zhang, J. Yang, J. Zheng, *Adv. Funct. Mater.* **2020**, *30*, 2004633.
[28] J. Yan, L. Cao, T. Luo, D. Qin, F. Hua, H. He, *Clin. Oral Investig.* **2023**, *27*, 6027.
[29] K. Yang, J. Shi, L. Wang, Y. Chen, C. Liang, L. Yang, L.-N. Wang, *J. Mater. Sci. Technol.* **2022**, *99*, 82.
[30] D. Dai, D. Li, C. Zhang, *Biomater. Sci.* **2023**, *11*, 4859.
[31] L. Memè, V. Notarstefano, F. Sampalmieri, G. Orilisi, V. ATR-FTIR, *Materials* **2021**, *14*, 818.
[32] O. H. Malik, A. McMullin, D. T. Waring, *Dent. Update* **2013**, *40*, 203.
[33] D. Łysik, K. Niemirowicz-Laskowska, R. Bucki, G. Tokajuk, J. Mystkowska, *Int. J. Mol. Sci.* **2019**, *20*, 3199.
[34] J. A. Lemos, S. R. Palmer, L. Zeng, Z. T. Wen, J. K. Kajfasz, I. A. Freires, J. Abranches, L. J. Brady, *Microbiol. Spectr.* **2019**, *7*, https://doi.org/10.1128/microbiolspec.GPP3-0051-2018
[35] S. Yang, J. Zhang, R. Yang, X. Xu, *Pathogens* **2021**, *10*, 1540.
[36] W. H. Bowen, R. A. Burne, H. Wu, H. Koo, *Trends Microbiol.* **2018**, *26*, 229.
[37] J. T. Poolman, A. S. Anderson, *Expert Rev. Vacc.* **2018**, *17*, 607.
[38] J. L. Lister, A. R. Horswill, *Front. Cell Infect. Microbiol.* **2014**, *4*, 178.
[39] S. Chen, L. Li, C. Zhao, J. Zheng, *Polymer* **2010**, *51*, 5283.